Proceedings of ASME Turbo Expo 2016: Turbomachinery Technical Conference and Exposition
GT2016
June 13 – 17, 2016, Seoul, South Korea

GT2016-57685

RAPID PRELIMINARY COMBUSTOR DESIGN USING A FLOW NETWORK APPROACH

B. du Toit
Flownex
24 Totius Street
Potchefstroom
2531
South Africa
bennie.dutoit@flownex.com

S. Theron
Phoenix Analysis & Design Technologies
7755 S. Research Dr.
Suite 110
Tempe, AZ 85284
USA
stephen.theron@padtinc.com

ABSTRACT

Preliminary combustor design usually requires that an extensive number of geometrical and operational conditions be evaluated and compared. During this phase important parameters the designer sought after are typically the mass flow rate distribution through air admission holes, associated pressure losses as well as liner wall temperatures. The process is therefore iterative in nature and can become expensive in terms of engineering analysis cost considering the time required to build and execute 3D CFD models. Network codes have the potential to fill the gap during this stage of the design since they can be setup and solved in timeframes that are orders of magnitude less than comprehensive CFD models, essentially leading to cost savings since overall less time is spent on 3D simulations and rig tests. An additional advantage using this approach is that results from the network solution can be applied as boundary conditions to subsequent more detailed 3D models.

In this study a commercial flow network tool, Flownex®, was used to model a complete combustor including flow distribution, combustion and heat transfer. The integrated mass, momentum and energy balance is solved using the continuity, momentum and energy equations applied to nodes and elements. These nodes and elements are the modular building blocks, typically semi-empirical and allow users to either select appropriate built-in correlations, or to define using specific equations through scripting. Flow equations are fully compressible and applied to the gas mixture. The chemical composition of the reactants forming during combustion as well as the adiabatic flame temperature is determined from the NASA CEA package incorporated into the solution. Heat transfer mechanisms included in the model are gas-surface radiation, film convection, forced convection in ducts, surface-surface radiation, and 2D axially-symmetric conduction through solid walls. Results produced from the network were compared with test data obtained from the NASA E3 development combustor. Overall good agreement resulted, showcasing the success of the approach followed.

INTRODUCTION

Typical preliminary combustor designs are carried out using an empirical approach that is geometrically inflexible and therefore very limited in application. Convergence problems may result with even small changes in geometry and/or boundary inputs. These tools are usually developed in-house in most companies and require specialist engineers for operation, maintenance and quality-, configuration- and data control. Additional drawbacks of some of these methods include assuming an incompressible flow field and a solution restricted to procedural solving techniques.

Improvements on the fully empirical approach was realized by Gouws [1] when he applied the commercial flow network solver, Flownex®, to obtain the mass flow rate distribution and pressure loss through the combustor. This approach entails combining and configuring modular flow entities, such as restrictors and duct components, to represent the flow path throughout the combustor. All these flow entities are based on fundamental one-dimensional equations for conservation, and supplemented by empirical information in the form of discharge coefficients for restrictors and frictional resistance correlations for ducts. These components therefore employ a semi-empirical

approach. In contrast with traditional fully empirical approaches, the flow network approach, through implementing modular building blocks to discretize the flow field, obtain a solution that is much more flexible in terms of geometrical changes and also independent of a particular solution procedure. A further benefit was that the flow field equations automatically became fully compressible. Despierre [2] also employed the Flownex® network solver to his genetic for preliminary combustor design.

In this paper the flow network approach to modelling the flow distribution in combustors was further expanded by developing a similar discretized network approach for heat transfer rate and temperature distribution inside the combustor flow paths as well as solid structures interacting with the fluid temperature field. This was achieved through defining and deriving heat transfer rate equations for all types of heat transfer mechanisms inside the combustor, to be used as primary building blocks in creating the heat transfer network. The mechanisms are gas-surface radiation, film convection, radial and axial conduction, surface-surface conduction and forced convection inside ducts. These mechanisms connect temperatures in either the flow network and/or heat transfer network with each other, resulting in a matrix of temperatures. The complete discretization of the temperature field in fluid and solid control volumes is an enhancement of the model presented by Gouws [1], whom had to revert to fully empirical modelling techniques for gas-surface radiation and film cooling heat transfer mechanisms.

In addition to this and to allow flexibility in terms of alternative fuel types and air-fuel ratios, the solution was also coupled to the NASA CEA package for modelling the combustion process itself and ultimately allow for automatic calculation of product gas composition and flame temperature given the reactant flow rates and temperatures.

Coupling the conjugate flow and heat transfer network with the combustion model enables the integrated simultaneous solution in a network solver such as Flownex®, giving the resulting flow distribution as well as liner wall temperatures.

NOMENCLATURE

Variables

A	Area / Coefficient
D	Diameter
E_b	Black body emissive power
F	View factor
f	Friction factor
H	Hydrogen mass fraction in percent
h	Convection coefficient / Enthalpy
J	Radiosity
k	Conductivity
L	Parameter to account for luminosity of soot particles / Length
L_b	Mean beam length
$\dot{m}$	Mass flow rate
m	Blow ratio
Nu	Nusselt number
p	Pressure
Pr	Prandtl number
$\dot{Q}$	Heat transfer rate
q	Fuel-air ratio
Re	Reynolds number
r	Radius
s	Slot height
T	Temperature
t	Slot lip thickness
V	Velocity
x	Distance from cooling slot source
α	Absorptivity
σ	Stefan-Boltzmann constant
ε	Emissivity
η	Film effectiveness
μ	Viscosity
ρ	Density
τ	Shear stress

Subscripts

a	Property of coolant air
ad	Adiabatic property
$cond$	Conduction
$conv$	Forced convection in a duct
e	Exiting flow/heat resistance element
f	Property of mainstream bulk fluid conditions
$film$	Film convection
i	Generic flow/solid node
in	Inflow flow/heat resistance element
j	Neighbouring node
k	Generic flow/heat resistance element
r	Radial direction/coordinate
rad	Radiation
s	Property at coolant air slot
w	Property at the wall
x	Property evaluated at distance x
z	Axial coordinate/direction
0	Stagnation property
1	Node/Surface 1
2	Node/Surface 2

NETWORK APPROACH

The so-called flow network modelling technique is a well-known concept throughout the spectrum of engineering industries. Applied to a piping system for instance it involves the representation of the flow system as a network of flow paths and components for the prediction of system-wide flow and bulk pressure distribution. Flow network modelling techniques is very efficient in terms of engineering hours required for model definition, solution and examination. In typical flow problems the system is modelled using conservation equations for mass, momentum and energy applied to individual components, leading to a matrix of dependencies. In most cases some form of empirical input is required to close the system of equations, as for example the friction factor correlation for piping systems.

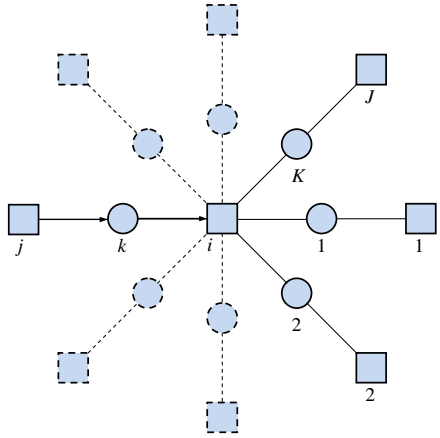

Figure 1: Nodes and elements in the flow network

Consider the flow network modelling technique applied to a generic junction *i* of ducting and restrictor elements 1...*K* inside the flow field in the combustor (Figure 1). Junction *i* is connected to neighbouring junctions 1...*J* via neighbouring elements 1...*K* . The junction is referred to as the node, while elements connect between an upstream and downstream node. Following a staggered grid approach one may apply continuity and energy conservation to the node while momentum equations are applied to the elements. From continuity applied to Node *i* and considering only steady-state flow:

$$\sum_k \dot{m}_k = 0 \qquad (1)$$

Pressure is related to flow rate through the element momentum conservation equation. This is element type specific. For a duct element between nodes *j* and *i*:

$$p_j - p_i = \frac{f_k L_k}{D_k}\frac{1}{2}\rho_k V_k^2 + \rho_i V_i^2 - \rho_j V_j^2 \qquad (2)$$

The shear stress at the pipe wall is related to the friction factor according to the Darcy-Weisbach definition in this case, $\tau_w = \frac{1}{8} f\left(\rho V^2\right)$. Eq. (2) holds for steady-state horizontal flow.

In the absence of heat transfer between nodes in the flow network, the conservation of energy to generic Node *i* in Figure 1 is represented by:

$$\sum_{in} \dot{m}_{in} h_{0,in} = \sum_e \dot{m}_e h_{0,e} \qquad (3)$$

This solution is frequently referred to as the cold flow case since it gives the flow distribution inside the combustor without combustion.

In order to allow for modelling the heat transfer between solids, solid surfaces and the fluid, the solid surfaces and solid control volumes needs to be connected to the flow network nodes as well as each other. To this end we distinguish between a flow node, like generic Node *i* above, and a solid node, which represents the solid control volumes and surfaces inside the liner and annulus walls. All flow nodes in the network will feature in the temperature matrix, though no solid node will feature in the pressure matrix.

Following the same approach as was done for the generic flow Node *i*, the equation for the conservation of energy can be applied to generic solid Node *i* in Figure 2 as follows:

$$\sum_k \dot{Q}_{in} = \sum_k \dot{Q}_e \qquad (4)$$

The heat transfer entering or leaving through heat resistance element *k* is then categorized as one of the following six heat transfer mechanisms: gas-surface radiation $\dot{Q}_{rad,f}$; film convection $\dot{Q}_{film}$; forced convection in a duct $\dot{Q}_{conv}$; radial conduction $\dot{Q}_{cond,r}$; axial conduction $\dot{Q}_{cond,z}$; or surface-surface radiation $\dot{Q}_{rad,s}$.

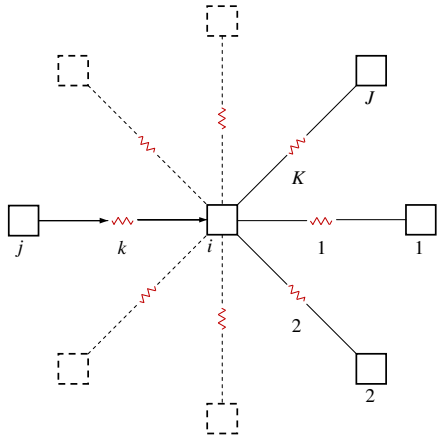

Figure 2: Nodes and heat resistances in the heat transfer network

For flow nodes Eq. (4) applies but with the addition of energy leaving or exiting the control volume through mass flow paths resulting from the continuity equation:

$$\sum_{in} \dot{m}_{in} h_{0,in} + \sum_{k} \dot{Q}_{in} = \sum_{e} \dot{m}_{e} h_{0,e} + \sum_{k} \dot{Q}_{e} \qquad (5)$$

Another difference between flow nodes and heat transfer nodes is that flow nodes never contain radial or axial conduction, or surface-surface radiation. In the section to follow the various heat transfer mechanisms will be related to the nodal temperatures.

HEAT TRANSFER MECHANISMS

A section of the combustor at an arbitrary cooling slot exit is shown in Figure 3. The spatial discretization for both the flow and heat transfer network is illustrated in the figure. The liner is heated through the radiation of heat resulting from the combustion in the main flow path. The cooling air exiting the slot in turn cools the liner through convection heat transfer between the liner surface and the jet boundary layer formed on its surface. The figure shows two increments in the axial direction following the slot exit (Flow and liner discretization in the axial direction coincides). The liner is further divided in two increments in the radial direction with the particular nodal temperatures located at the two surfaces of the liner. Additional increments may be added for finer discretization in the radial direction. The liner discretization leads to a two-dimensional grid where conduction is accounted for in both the radial as well as axial conduction elements, as illustrated in the figure. At the outer surface of the liner heat is transferred to the annulus air through forced convection in a duct, as well as surface-surface radiation between the liner and annulus walls. The annulus wall is incremented similar to the liner wall and also accounts for two-dimensional heat conduction.

Following combustion heat is transferred between the participating gasses in the main flow path and the liner wall via gas-solid radiation. Gasses such as water vapour and carbon dioxide (heteropolar gasses), take part in the radiation mechanism of heat exchange as they emit and absorb radiation at certain bands of wavelengths. This is referred to as non-luminous radiation. Luminous radiation on the other hand represents the radiation exchange between solid soot particles and the surface. The net radiant heat transfer rate between participating gasses and an enclosed surface of a black body can be calculated from the bulk fluid properties as follows [3]:

$$\dot{Q}_{rad,f} = \sigma A \left(\varepsilon_f T_f^4 - \alpha_f T_w^4 \right) \qquad (6)$$

The emissivity of the gas is calculated at the existing gas temperature, while the absorptivity of the gas is calculated at the wall temperature; since the gas is absorbing thermal radiation given off by the wall at the wall temperature. For surfaces that are not black, the surface emissivity is less than unity. This is accounted for by modifying Eq. (6) with the surface emissivity as follows [4]:

$$\dot{Q}_{rad,f} = \sigma A \left\{ \frac{\varepsilon_w}{1-(1-\varepsilon_w)(1-\alpha_f)} \right\} \left(\varepsilon_f T_f^4 - \alpha_f T_w^4 \right) \qquad (7)$$

The gas emissivity and wall absorptivity are empirical inputs required to solve the gas-surface radiation. For example, consider the correlation given by Lefebvre [5]:

$$\varepsilon_f = 1 - \exp\left(-290\, pL \left(qL_b \right)^{0.5} T_f^{-1.5} \right) \qquad (8)$$

$$\frac{\alpha_f}{\varepsilon_f} = \left(\frac{T_f}{T_w} \right)^{1.5} \qquad (9)$$

The variable L accounts for luminosity of the mixture due to soot particles, and is dependent on the hydrogen content as follows:

$$L = \frac{336}{H^2} \qquad (10)$$

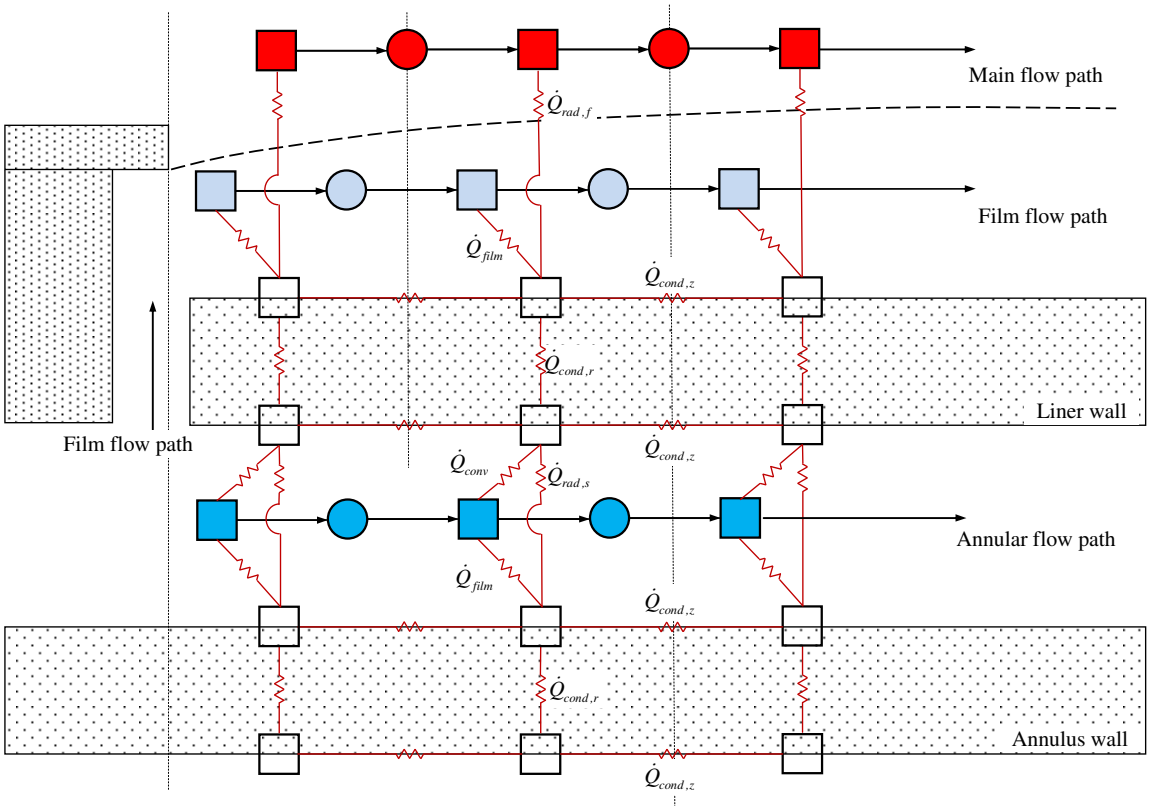

Figure 3: Conjugate flow and heat transfer network at a cooling slot exit

Calculating convection heat transfer between the liner wall and the coolant in contact with it requires special consideration compared to conventional convection heat transfer in ducts for instance. In the latter case it suffices to use the relevant fluid temperatures and the convection resistances on the two sides. Film convection however introduces a third temperature into the equation in the form of the definition of the film effectiveness and the adiabatic wall temperature $T_{w,ad}$. The effectiveness of the film at a distance x from slot exit is defined in terms of the temperature that a liner with zero flame radiation and zero external cooling will reach for given gas and coolant flow temperatures as follows:

$$\eta = \frac{T_f - T_{w,ad}}{T_f - T_a} \tag{11}$$

Empirical correlations are used to calculate the film effectiveness. From Lefebvre for thin-lipped slots $\left(\frac{t}{s} < 0.2\right)$ and $0.5 < m < 1.3$:

$$\eta = 0.6\left(\frac{x}{ms}\right)^{-0.3}\left(Re_s \frac{m\mu_a}{\mu_f}\right)^{0.15} \tag{12}$$

For thin-lipped slots and $1.3 < m < 4$, one of the following three equations are used depending on the value of $\frac{x}{ms}$:

For $\frac{x}{ms} < 8$ and $1.3 < m < 4$:

$$\eta = 1.0 \tag{13}$$

For $8 < \frac{x}{ms} < 11$ and $1.3 < m < 4$:

$$\eta = \frac{1}{0.6 + 0.05\left(\frac{x}{ms}\right)} \tag{14}$$

For $\frac{x}{ms} > 11$ and $1.3 < m < 4$:

$$\eta = 0.7\left(\frac{x}{s}\right)^{-0.3}\left(Re_s \frac{\mu_a}{\mu_f}\right)^{0.15} m^{-0.2} \tag{15}$$

For thick-lipped slots $\left(\frac{t}{s} > 0.2\right)$ and $0.5 < m < 1.3$:

$$\eta = 1.1 m^{0.65} \left(\frac{\mu_a}{\mu_f}\right)^{0.15} \left(\frac{x}{s}\right)^{-0.2} \left(\frac{t}{s}\right)^{-0.2} \quad (16)$$

For thick-lipped slots and $1.3 < m < 4$:

$$\eta = 1.28 \left(\frac{\mu_a}{\mu_f}\right)^{0.15} \left(\frac{x}{s}\right)^{-0.2} \left(\frac{t}{s}\right)^{-0.2} \quad (17)$$

Lefebvre & Ballal based their equations on a jet model rather than a developed turbulent boundary layer. This is especially true in the near slot region (smaller values of $\frac{x}{s}$), where the boundary layer is not yet developed, and also particularly in situations where the velocity of the cooling air is significantly higher than that of the main stream . For boundary-layer type film flow a correlation such as that published by Wieghardt can be used [6]:

$$\eta = 21.8 \left(\frac{x}{ms}\right)^{-0.8} \quad (18)$$

The film effectiveness and adiabatic wall temperature are related to the convection heat transfer rate from the inner liner wall temperature $\left(T_w\right)$ and the air flowing in the adjacent film as follows:

$$\dot{Q}_{film} = hA\left(T_w - T_{w,ad}\right) \quad (19)$$

To calculate *h* any appropriate correlation for convection coefficient over a flat plate can be used. In general:

$$Nu_x = C\, Re_x^m\, Pr_a^n \quad (20)$$

As input the film convection resistance element also needs the distance *x* form the slot exit at both ends, since the correlations are dependent on these. Furthermore the cooling air and hot gas temperature nodes at cooling slot exit needs to be specified to conform to the definition of effectiveness.

Radiation heat-exchange in a two-surface enclosure of two diffuse, gray surfaces can be expressed as [3]:

$$\dot{Q}_{rad,s} = \frac{\sigma\left(T_1^4 - T_2^4\right)}{\frac{1-\varepsilon_1}{\varepsilon_1 A_1} + \frac{1}{A_1 F_{12}} + \frac{1-\varepsilon_2}{\varepsilon_2 A_2}} \quad (21)$$

Eq. (21) holds when the view factor between the two surfaces is unity, i.e. it is a series combination of two surface resistances and one geometrical resistance. When the heat transfer is between multiple surfaces then one have to model the surface and geometrical components individually in a network format. The net radiative heat transfer rate from surface 1 is given as:

$$\dot{Q}_{rad,s} = \frac{E_{b1} - J_1}{\frac{1-\varepsilon_1}{\varepsilon_1 A_1}} \quad (22)$$

The geometrical resistance between surface 1 and 2 is represented by:

$$\dot{Q}_{rad,s} = \frac{J_1 - J_2}{\frac{1}{A_1 F_{12}}} \quad (23)$$

The conduction heat transfer rate in the radial direction between r_1 and r_2 can be calculated from Fourier's law of conduction:

$$Q_{cond,r} = \frac{k 2\pi \Delta x}{\ln\left(\frac{r_2}{r_1}\right)}\left(T_1 - T_2\right) \quad (24)$$

For an axial conduction heat resistance element:

$$\dot{Q}_{cond,z} = \frac{k\pi\left(r_2^2 - r_1^2\right)}{\Delta x}\left(T_2 - T_1\right) \quad (25)$$

Convection heat transfer between the air flowing in the annulus and the liner surface is represented by Newton's law of cooling:

$$\dot{Q}_{conv} = hA\left(T_w - T_{an}\right) \quad (26)$$

Any appropriate correlation for forced convection inside ducts can be used in Eq. (26). Consider as example the Gnielinski correlation:

$$Nu = \frac{\frac{f}{8}\left(Re - 1000\right) Pr}{1 + 12.7\left(\frac{f}{8}\right)^{1/2}\left(Pr^{2/3} - 1\right)} \quad (27)$$

Eq. (26) also holds for convection to the annulus outer surface but with appropriate temperatures.

COMBUSTION CALCULATION

The product gas mole fractions and adiabatic flame temperature of the combustion process is calculated with the NASAGlenn Chemical Equilibrium Program CEA2 (also referred to as the Gordon-McBride program) [7]. This program will run in the background and without the user knowing it. Flownex® generates an input file for the Gordon-McBride program and populates the input file by retrieving the reaction pressure, inlet temperature and the mass fractions of the reactants with their reactant names from the upstream node.

The Gordon-McBride program uses this generated input file to generate the output file. Flownex® applies the calculated mass fractions of the products and the gas mixture temperature to the downstream node.

The Gordon-McBride program uses its own internal library to calculate the properties of the reactants and products, each with its own unique fluid code. This fluid code identifies the fluids in the Gordon-McBride program's input and output files. The fluid code related to a specific fluid in the Gordon-McBride program is mapped to its counterpart in Flownex®, thereby enabling information exchange.

It should be noted that the Gordon-McBride program does not account for geometry of the combustor, thus the product gas temperature is calculated by assuming there is no radiation or heat transfer, i.e. adiabatic. This entire network is therefore modelled in Flownex®. Equally all pressure losses and flow rates are all treated in the Flownex® flow network.

NETWORK MODEL BACKGROUND

In the 1980s, NASA funded the Energy Efficient Engine program to demonstrate fuel efficient designs for the next generation of transport aircraft. The purpose of the E3 Program was to develop and demonstrate the technology for obtaining higher thermodynamic and propulsive efficiencies in advanced, environmentally acceptable turbofan engines for possible use in future commercial transport aircraft. While the E3 engine was never in production, the technology developed during the program underpins many of the current generation of gas turbine engines. The NASA report [8] that summarizes the results of the detailed design and analysis efforts of the advanced double-annular combustion system for General Electric's Energy Efficient Engine was used to set up a benchmark to evaluate the flow network approach described in this paper.

The network geometry was not obtained from original CAD models but was recreated through the vectorization of drawings, from the aforementioned NASA report, using a 3D modeling software called SpaceClaim. While these sources are not as reliable as having the actual CAD representations, they do provide adequate information to analyze the system.

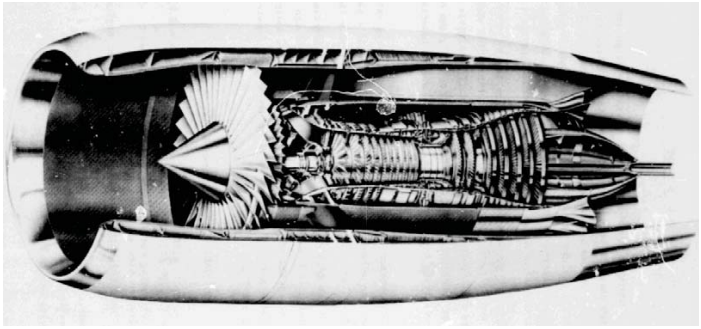

Figure 4: Energy Efficient Engine developed by General Electric

The availability of geometry is always a major restraint to testing and improving simulation codes and approaches in a full system environment. While previous studies have been carried out to validate the flow network approach reported here, they used proprietary geometries that could not be further disseminated.

NETWORK SIMULATION CASES

All simulation cases carried out in Flownex® were compared to E3 baseline development combustor test results obtained from full-annular combustor component development testing. Key features of the development combustor are shown in Figure 5.

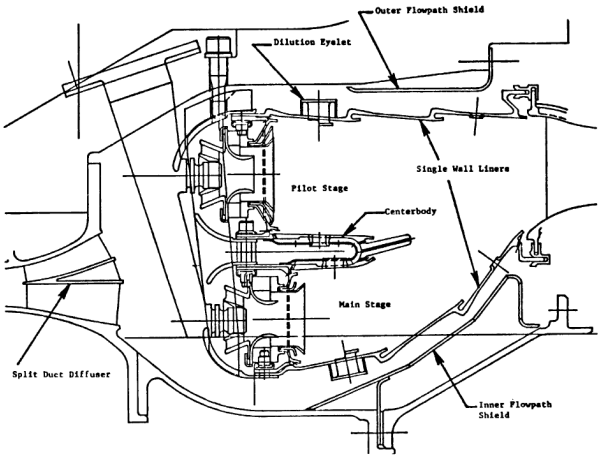

Figure 5: E3 Full-annular development combustor

The development combustor consists of a double-annular dome assembly separated by a center body. Each dome has 30 equally spaced swirl-cup assemblies. The development combustor liners are a conventional machined ring film cooled design.

Testing was conducted in a full-annular, high pressure test rig specifically designed to house the E3 combustor. The full-annular combustor test rig exactly duplicates the engine combustor aerodynamic flow path and envelope dimensions.

Test Point	Inlet Pressure [psi]	Inlet Temperature [K]	Combustor Exit Mass Flow [pps]	Overall Fuel Air Ratio	Pilot/Total Fuel Mass Flow
1	174.9	637	57.1	0.0171	0.50
2	240.04	700	66.25	0.0173	0.40
3	240.04	745	68.65	0.0208	0.41
4	240.7	781	68.33	0.0229	0.35
5	241.3	788	67.78	0.0233	0.35
6	241.5	814	67.48	0.0246	0.40

Table 1: Combustor operating conditions

The purpose of the testing was to evaluate the baseline combustor design for emissions, pressure drop, and metal temperature characteristics at combustor operating conditions along the E3 design operating cycle.

Select points and corresponding operating conditions evaluated in these tests were used as boundary condition in the network model. The test points can be viewed in Table 1.

While most of the combustor geometry is well described some uncertainties were encountered with regards to the effective area of several air admission holes. Since the pressure and flow relationships are well understood and the purpose of the study is to investigate the heat transfer mechanisms, it was considered acceptable to back engineer air admission hole areas to obtain a known combustor air flow rate distribution and pressure drop. The air flow distribution as designed for 5.5% overall combustor pressure drop can be seen in Figure 6 below.

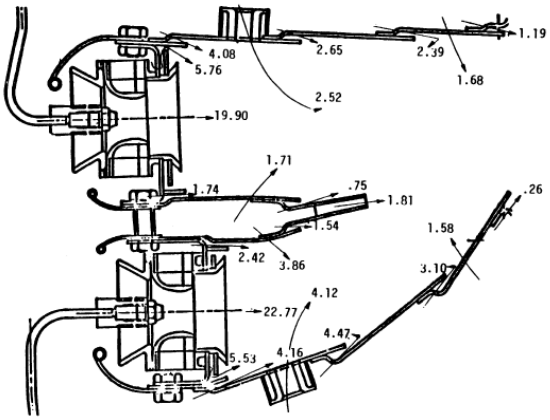

Figure 6: Combustor air flow distribution

NETWORK MODEL

The combined flow and heat transfer network, which comprised of 162 nodes and 478 elements can be seen in Figure 7. A more detailed section of the network at a cooling slot exit is shown in Figure 8. Steady-state solutions are obtained in a few seconds.

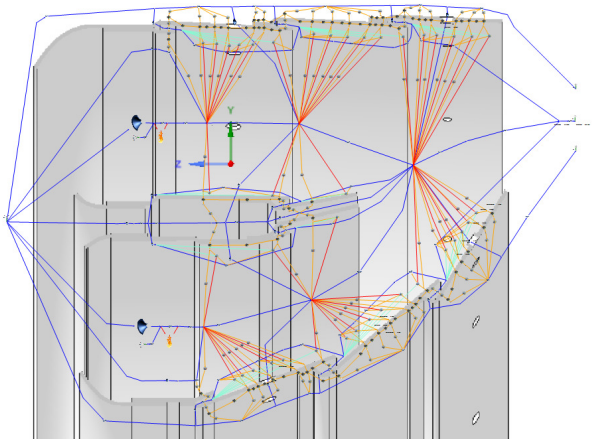

Figure 7: Flownex® network model overlaid on 2D image of CAD model

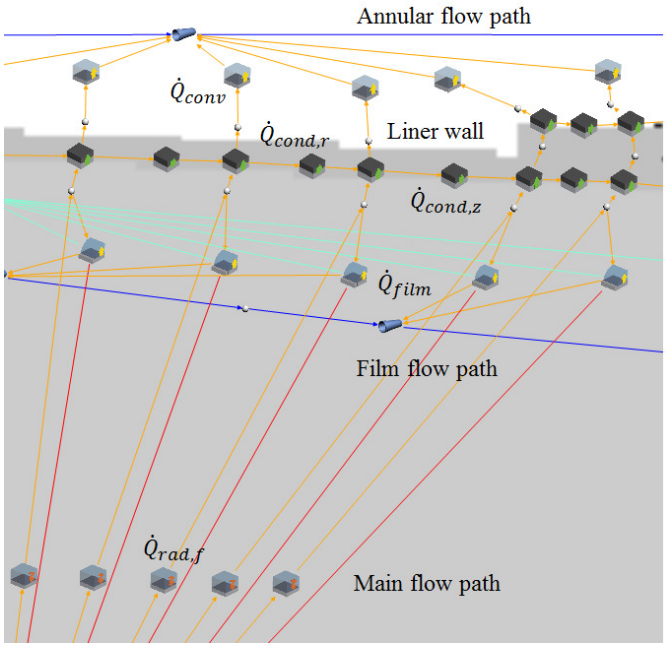

Figure 8: Flownex® network at a cooling slot exit

NETWORK RESULTS

The outer liner hot side metal temperature profile resulting from the Flownex® network model for each test point, previously described in Table 1, can be seen in Figure 9 below:

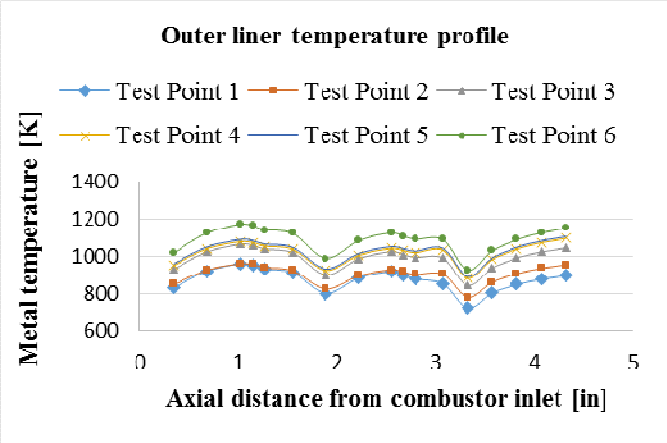

Figure 9: Simulation outer liner temperature profile

As expected the lowest temperatures are observed closest to film cooling slots. As the axial distance from a slot increases and film efficiency decreases, an increase in metal surface temperature follows.

Temperature results from the simulation were compared to temperatures measured at two of the thermocouples on the test rig. The results can be viewed in Figures 10 – 15. Overall the simulation results show good agreement with test data. Percentage errors in liner wall temperatures are in the range 1% - 13%.

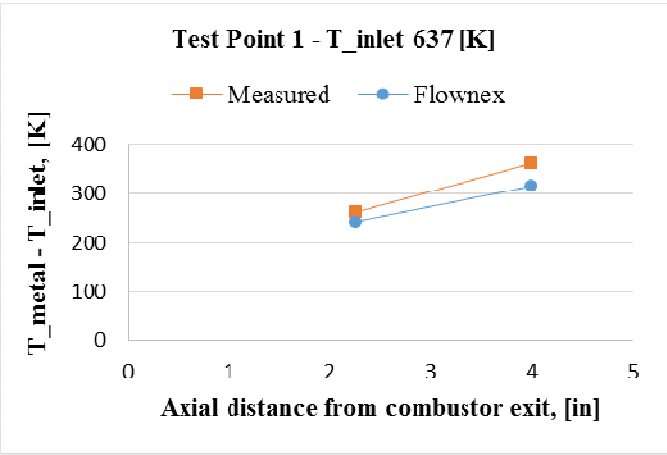

Figure 10: Measured outer liner metal temperature versus simulation results – test point 1

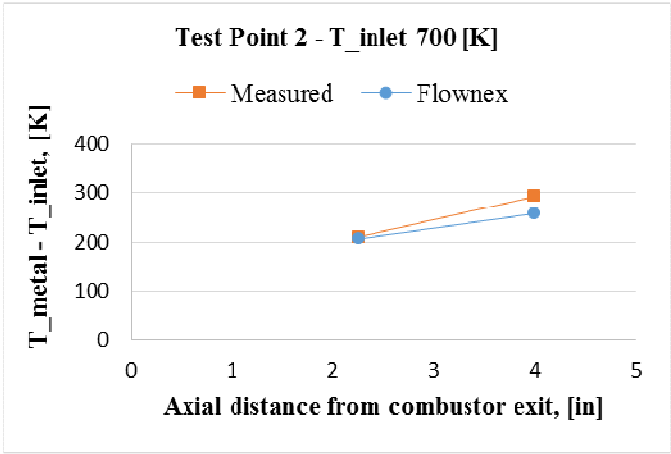

Figure 11: Measured outer liner metal temperature versus simulation results – test point 2

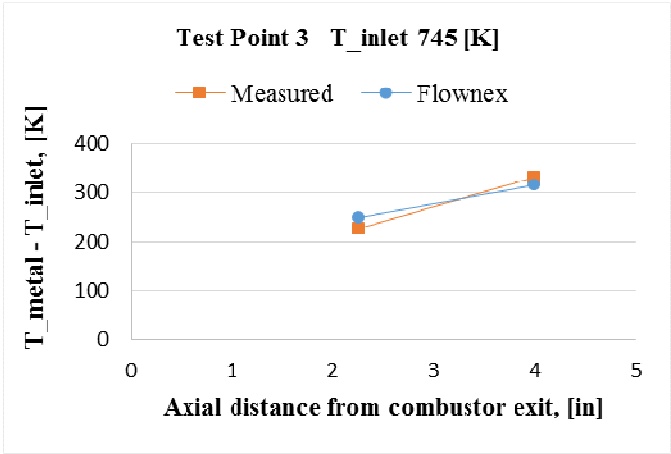

Figure 12: Measured outer liner metal temperature versus simulation results – test point 3

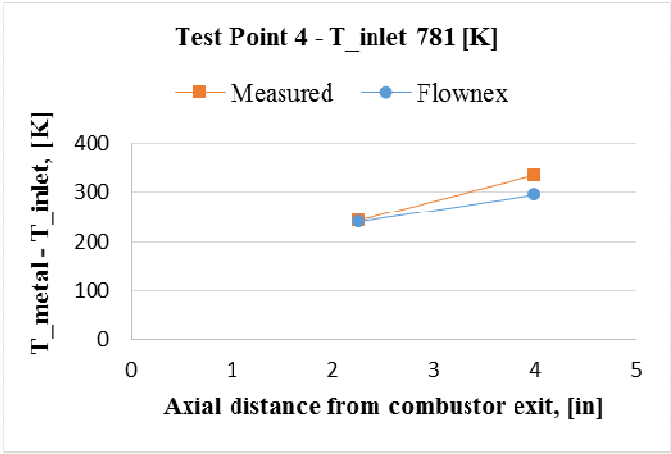

Figure 13: Measured versus simulation metal temperature – test point 4

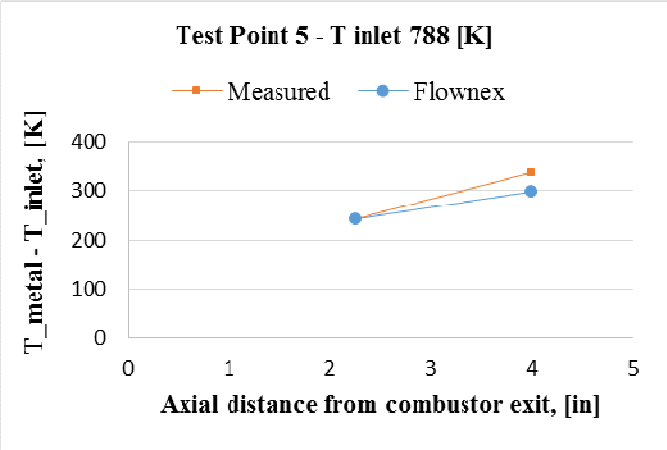

Figure 14: Measured outer liner metal temperature versus simulation results – test point 5

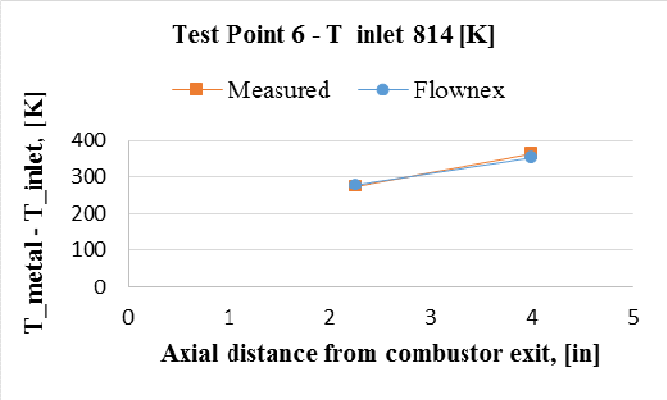

Figure 15: Measured outer liner metal temperature versus simulation results – test point 6

CONCLUSION

In this study a commercial flow network tool, Flownex®, was used to model a complete combustor including flow distribution, combustion and heat transfer. The integrated mass, momentum and energy balance is solved using the continuity, momentum and energy equations applied to nodes and elements.

Ultimately the objective of using the flow network approach instead of 3D CFD is to reduce engineering and design costs during initial and preliminary design stages through reducing the amount of CFD runs and rig tests required. The flow network approach has already been proven and is frequently used to predict flow distribution patterns and pressure losses in combustors. In this paper the network approach was extended to also include for the various heat transfer mechanisms typically found in a combustor, thereby ending with a coupled, conjugate flow and heat transfer network. The network, coupled to a comprehensive combustion calculation, solves within seconds and also maximizes flexibility in terms geometrical inputs and boundary conditions, compared to fully empirical models.

A benchmark model was setup and compared with test data. Overall the results show good agreement, with simulation results showing the same trends as measured data. While minor deviation was observed in some areas, the approach employed is flexible enough for future refinements to be made to the modelling assumptions and network layout.

REFERENCES

[1] Gouws, J.J., Morris, R.M. & Visser, J.A. 2006. Modelling of a gas turbine combustor using a network solver. *South African Journal of Science.*, November/December 2006.

[2] Despierre, A, Stuttaford, P.J. & Rubini, P.A. 1997. Gas turbine combustor design using genetic algorithms. *Int. Gas Turbine and Aeroengine Congress & Exhibition, Orlando, Florida, June 2-5, 1997*. ASME Paper 97-GT-72.

[3] Incropera, P.I. & DeWitt, D.P. 1996. Fundamentals of Heat and Mass Transfer. New York : John Wiley & Sons, Inc. 886 p.

[4] VDI Heat Atlas. 2010. Berlin : Springer-Verlag, 1551 p.

[5] Lefebvre, A.H. & Ballal, D.R. 2010. Gas Turbine Combustion. Boca Raton : CRC Press. 537 p.

[6] Wieghardt, K. 1946. Hot Air Discharge for De-Icing, *Air Material Command, AAF*
Trans. No. F-TS-919-RE.

[7] Gordon, S., McBride, B.J. 1994. Computer Program for Calculation of Complex Chemical Equilibrium Compositions and Applications. *NASA Reference Publication 1311, Part I.*

[8] Burrus, D.L., et al. 1984. Energy Efficient Engine (E3) Combustion System Component Technology Performance Report. *NASA contract report – 168274*